Available online at www.sciencedirect.com

SCIENCE DIRECT®

Lithos 83 (2005) 299–316

LITHOS

www.elsevier.com/locate/lithos

Crustal assimilation in basalt and jotunite: Constraints from layered intrusions

Christian Tegner[a,*], J. Richard Wilson[a], Brian Robins[b]

[a]*Department of Earth Sciences, University of Aarhus, C. F. Møllers Allé 110, DK-8000 Aarhus, Denmark*
[b]*Department of Earth Science, University of Bergen, Allégt. 41 N-5007 Bergen, Norway*

Received 5 December 2003; accepted 18 February 2005
Available online 25 April 2005

Abstract

To constrain the amount and rate of crustal contamination that is possible in basaltic and jotunitic magma, and to gain an insight into the physical and thermal processes of assimilation in crustal magma chambers, we have modelled published Sr and Nd isotopic data from three layered intrusions. Well-exposed sequences of cumulates with no evidence of magma recharge provide direct records of concurrent assimilation and fractional crystallization (AFC). The key to the modelling is that F, the mass fraction of magma remaining in the chamber, can be estimated from the thicknesses of the studied cumulate sequences. This allows AFC model curves to be fitted to the isotopic data by varying $\boldsymbol{r}$, the ratio of the rate of mass assimilated to the rate of mass crystallized. The results of modelling show that $\boldsymbol{r}$ is nearly constant in 800 to 2000 m thick sequences of cumulates displaying up-section decreases in anorthite content of plagioclase, increases in whole-rock Sr_0 (initial $^{87}Sr/^{86}Sr$) and decreases in whole-rock εNd_0 (initial εNd). The $\boldsymbol{r}$-values of the layered sequences range from ~0.12 in the Fongen–Hyllingen Intrusion, over 0.20 in the Bjerkreim–Sokndal Intrusion, to 0.27 in the Hasvik Intrusion. The total amount of assimilation, the *bulk crust/magma ratio*, reaches values of 0.08, 0.19 and 0.28 at the level of the most contaminated samples after 60% to 80% crystallisation, whereas the *instantaneous crust/magma ratio* of the most contaminated magmas were respectively 0.14, 0.46, and 0.70, for the three intrusions.

Innumerable country rock xenoliths occur in the three layered intrusions and played a crucial role in the assimilation process. The xenoliths spalled off the roofs of the magma chambers during magma emplacement and their initial temperature and composition relate to $\boldsymbol{r}$ in the intrusions. In the Hasvik Intrusion ($\boldsymbol{r}=0.27$), the initial temperature of the country rocks was ~450 °C and the xenoliths were fusible metasediments and therefore produced a high fraction of partial melt that could be assimilated. In the Bjerkreim–Sokndal Intrusion ($\boldsymbol{r}=0.20$), the country rocks were initially at temperatures of 640–880 °C but included both refractory massif-type anorthosite and fusible gneisses. In the Fongen–Hyllingen Intrusion ($\boldsymbol{r}=0.12$), the country rocks were cooler (~300 °C) and the xenoliths include refractory metabasalt (dominant) and fusible metapelite. We argue that the refractory metabasalt and anorthosite xenoliths acted mainly as heat sinks, resulting in reduced $\boldsymbol{r}$-values in Fongen–Hyllingen and Bjerkreim–Sokndal Intrusions.

Heating of refractory and fusible xenoliths, and melting of fusible xenoliths absorbed sensible and latent heat of the magma. Energy-balanced modelling shows that up to 75% of the heat available was absorbed by xenoliths within the magma chambers, promoting higher rates of cooling and crystallisation than would have resulted from loss of heat to the envelope of country rocks

---

* Corresponding author. Tel.: +45 8942 2530; fax: +45 8942 2525.
E-mail addresses: christian.tegner@geo.au.dk (C. Tegner), jrw@geo.au.dk (J.R. Wilson), brian.robins@geo.uib.no (B. Robins).

0024-4937/$ - see front matter
doi:10.1016/j.lithos.2005.03.007

alone. The high ***r***-values reflect the amount of heat absorbed by heating and melting country rock within the magma chambers themselves, and their constancy reflects the ready availability of fusible xenoliths.

Keywords: Layered mafic intrusion; Crustal assimilation; Xenoliths; Hasvik; Fongen–Hyllingen; Bjerkreim–Sokndal, Norway

1. Introduction

Concurrent crustal assimilation and fractional crystallization (AFC) is recognised in virtually all mantle-derived magmas emplaced into the Earth's crust. For example, in the Oman ophiolite, the mid-ocean ridges, and the Skaergaard Intrusion, all previously thought to have negligible crustal contamination, recent isotopic and trace element investigations have demonstrated some assimilation of the local country rocks (Stewart and DePaolo, 1990; Michael and Cornell, 1998; Coogan et al., 2003). Crustal assimilation may significantly alter the composition of magmas, including their water and chlorine contents, resulting in significant changes in liquidus relations, liquid lines of descent, and, perhaps most importantly, the proportions and compositional variety of the differentiation products (Bowen, 1928; Wilcox, 1954; Taylor et al., 1979; Reiners et al., 1995).

The physical processes by which assimilation takes place and the amounts and rates of assimilation, however, remain at best loosely constrained. In the AFC formulation of DePaolo (1981), the ratio of the rate of mass assimilated to the rate of mass crystallized, ***r***, can only be determined if the fraction of the mass of magma remaining (F) can be estimated. This is commonly impossible in volcanic systems. Hence, a shortcoming of AFC modelling is that ***r*** normally has to be assumed.

Contamination of mantle-derived magmas takes place mainly in large crustal magma chambers. It is a consequence of coupling between the concurrent release of latent heat of crystallization and heat consumed in heating and melting country rocks (Bowen, 1928; DePaolo, 1981). Layered intrusions, which represent solidified magma chambers, often provide secular records of concurrent assimilation and fractional crystallization, as demonstrated by the inverse correlation of plagioclase compositions [An%=Ca/(Na+Ca)] and Sr_0 (initial $^{87}Sr/^{86}Sr$) (Fig. 1). In layered sections, the upward decrease in An% and the successive appearance of cumulus phases correlate with F. This applies both when the up-section decrease in An% is continuous and step-like. Layered intrusions therefore provide direct insights into AFC processes.

In this presentation we first review published estimates of ***r*** from thermodynamic models such as MELTS (Reiners et al., 1995), energy-constrained assimilation and fractional crystallization (EC-AFC; Spera and Bohrson, 2001), and a kinetic model for rates of mineral dissolution (Edwards and Russell, 1998). We then discuss the maximum rates and amounts of country rock assimilation that are possible in crustal magma chambers. Thirdly, we review and model published Sr- and Nd-isotopic data from the Bjerkreim–Sokndal, Fongen–Hyllingen and Hasvik layered intrusions with the aim of constraining ***r*** and the amount of assimilation. Finally, we discuss the physical

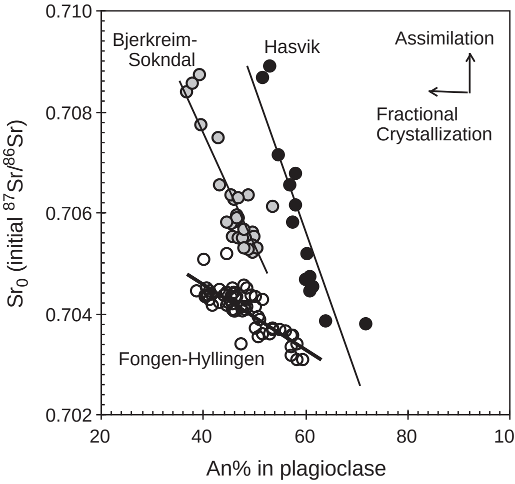

Fig. 1. Relationships between whole rock Sr_0 (initial $^{87}Sr/^{86}Sr$) and An% in plagioclase of sequences of cumulates formed by concurrent assimilation and fractional crystallization in large crustal magma chambers. The data shown are from the Bjerkreim–Sokndal (Nielsen et al., 1996), Fongen–Hyllingen (Sørensen and Wilson, 1995), and Hasvik layered intrusions, Norway. Modified from Tegner et al. (1999).

and geochemical limits and controls on $\boldsymbol{r}$, and point out the importance of country-rock xenoliths in promoting crustal contamination in magma chambers.

2. Nomenclature and definitions

The nomenclature and definitions used are given in Table 1. The *rate of assimilation* is normally expressed as the ratio of the rate of mass assimilated (dM_a) and rate of mass crystallized (dM_c) and denoted $\boldsymbol{r}$ (dM_a/dM_c) (DePaolo, 1981). The *amount of assimilation* may either be expressed as the ratio of the total mass assimilated (M_a) to the original magma mass (M_{om}), M_a/M_{om}, denoted the *bulk crust/magma ratio* of the entire system, or as the mass of assimilated material (M_{ia}) relative to the mass of the original magma remaining (M_{iom}) in the contaminated magma, denoted as the *instantaneous crust/magma ratio*.

Table 1
Nomenclature and definitions

Symbol	Definition	Unit
c_a	element concentration in the assimilated material	p.p.m.
c_m	element concentration in the magma	p.p.m.
C_{cr}	specific heat capacity of the country rock involved in AFC	J/kg per K
C_m	specific heat capacity of the magma	J/kg per K
D_e	effective bulk distribution coefficient of an element	
ΔT_m	the temperature drop of the magma during AFC	K
ΔT_{cr}	the temperature increase of the country rock during AFC	K
e_a	isotopic ratio of the assimilated material	
e_m	isotopic ratio of the magma	
E_L	proportion of energy lost to surrounding country rocks	
$1-E_L$	proportion of energy used to heat and melt M_{cr}	
F	mass proportion of magma remaining [M_m/M_{om}]	
L_c	latent heat of crystallization	J/kg
L_{cr}	latent heat of melting country rock	J/kg
M_{om}	mass of original magma	kg
M_{iom}	instantaneous mass of original magma in contaminated magma	kg
M_{cr}	mass of country rock involved in the AFC process	kg
M_a	mass of assimilated material (partial melt)	kg
M_{ia}	instantaneous mass of assimilated material in contaminated magma	kg
M_c	mass crystallized (cumulates)	kg
M_m	mass of magma in the chamber ($M_{om}+M_a\div M_c$)	kg
M_a/M_{om}	bulk crust/magma ratio	
M_{ia}/M_{iom}	instantaneous crust/magma ratio	
$\boldsymbol{r}=\mathrm{d}M_a/\mathrm{d}M_c$	ratio of the rate of mass assimilated to the rate of mass crystallized	

3. Constraints on the rate and amount of crustal assimilation

3.1. Thermodynamic models

Thermodynamic models of $\boldsymbol{r}$ and the *bulk crust/magma ratio* give widely differing results.

Using the MELTS formulation, Reiners et al. (1995) showed that for a primitive MORB magma at 1230 °C initially crystallizing olivine alone and assimilating a partial melt derived from metapelite that had an initial temperature of 400 °C, the rate of mass assimilated exceeds that of the rate of mass crystallized and $\boldsymbol{r}$ values are up to 1.5 (Fig. 2a). This is mainly a consequence of the steep liquidus surface that suppresses the rate of crystallization relative to temperature decrease. When this magma crystallizes Ca-rich pyroxene and plagioclase, the ratio of mass crystallized to original magma mass (M_c/M_{om}) is 0.09 and $\boldsymbol{r}$ drops to ~0.5 (Fig. 2a). In this simulation, the *bulk crust/magma ratio* is ~0.23 for M_c/M_{om} of 0.35 (Fig. 2b).

An example of a simulation using the computer program for energy-constrained assimilation and fractional crystallization (EC-AFC) provided by Spera and Bohrson (2001) is also shown in Fig. 2. For conditions identical to those above and assuming an equilibrium temperature of 1000 °C and a solidus temperature of 850 °C for the assimilated material, the EC-AFC simulation predicts that $\boldsymbol{r}$ remains zero for a prolonged interval of crystallization during which the country rock envelope is heated to its solidus temperature (Fig. 2a). Once assimilation of partial melts from the preheated thermal aureole commences at M_c/M_{om} of 0.35, $\boldsymbol{r}$ is initially 1.0 (Fig. 2a). With further crystallization $\boldsymbol{r}$ increases gradually to 2.9 at M_c/M_{om}

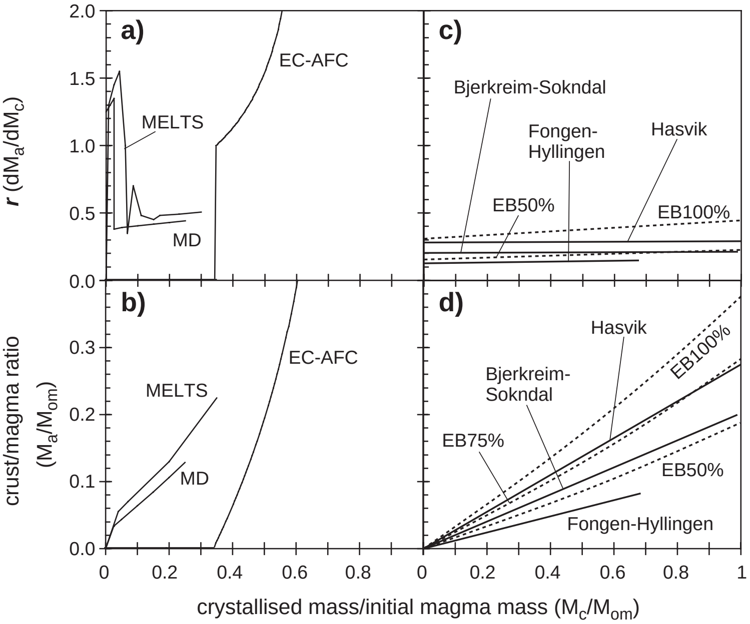

Fig. 2. (a) The ratio of the rate of assimilated mass to the rate of crystallized mass ($\mathrm{d}M_a/\mathrm{d}M_c$, or $\boldsymbol{r}$) for published AFC models. Shown are $\boldsymbol{r}$-values obtained from: (i) MELTS (Reiners et al., 1995) and EC-AFC (Spera and Bohrson, 2001) simulations for the assimilation of a partial melt of metapelite with an initial temperature of 400 °C into MORB magma with an initial temperature of 1230 °C; and (ii) a kinetic mineral dissolution model for the assimilated material in basaltic magma (denoted MD; Edwards and Russell, 1998). (b) Shows the *bulk crust/magma ratio* defined as the ratio of the mass assimilated to the mass of original magma (M_a/M_{om}) for the same simulations as in (a). (c) $\boldsymbol{r}$-values for: (i) Energy Balanced simulations (Eq. (1), see text) assuming that either *all* (EB100%), *three-quarter* (EB75%) or *half* (EB50%) of the energy released from the latent heat of crystallization and cooling is consumed in the assimilation process; and (ii) results of AFC modelling of Sr_0 and $\varepsilon\mathrm{Nd}_0$ presented in this contribution for thick layered cumulate sequences of the Fongen–Hyllingen, Bjerkreim–Sokndal and Hasvik intrusions.

of 0.61 where the simulation reached the equilibrium temperature and was terminated. This gradual increase in $\boldsymbol{r}$ is apparently a consequence of a decrease in the sensible heat required to heat the partial melt to the temperature of the magma, which of course decreases with crystallization. At a M_c/M_{om} of 0.61, the EC-AFC model predicts a *bulk crust/magma ratio* of 0.41 (Fig. 2b).

Edwards and Russell (1998) modelled $\boldsymbol{r}$ by combining a kinetic model predicting rates of mineral dissolution within the assimilated material with equilibrium thermodynamics. For primitive basaltic lava of the Iskut volcanic field, Canada, they calculated that $\boldsymbol{r}$ is above unity (1.3–1.4) in the high temperature crystallization interval (1210–1185 °C) where olivine is the only liquidus phase (Fig. 2a), a result similar to that of Reiners et al. (1995). After plagioclase starts crystallizing at M_c/M_{om} of 0.025, r drops to 0.39 and then increases gradually to 0.44 at M_c/M_{om} of 0.25 (Fig. 2a). The results of this simulation are qualitatively similar to Reiners et al. (1995).

3.2. Thermal constraints

In a magma chamber, heat is lost to the envelope of country rocks, any xenoliths that may be present and hydrothermal systems. In addition, heat may be absorbed by assimilation. If E_L is the proportion of energy lost to the envelope, the energy balance is:

$$(1-E_L)(M_{om}C_m\Delta T_m+M_cL_c)$$
$$=M_{cr}C_{cr}\Delta T_{cr}+M_aL_{cr}. \qquad (1)$$

The symbols are defined in Table 1. The left-hand side of the equation gives the total amount of heat not lost to the surrounding rocks and hence available for assimilation. The right-hand side of the equation is the heat required to heat the country rock involved in the assimilation process (M_{cr}) and the heat required to produce a partial melt of mass M_a that is assimilated, assuming constant latent heats of crystallisation and heat capacities. For metapelite, the mass fraction of partial melt (M_a/M_{cr}) is assumed to be 0.65 at 1000 °C (Vielzeuf and Holloway, 1988). The model thus assumes that 35% of the country rock mass involved in the assimilation process is preserved in the crystallized magma chamber as restite material, for example as xenocrysts or recrystallized xenoliths. If it is then assumed that the crystallized mass relates linearly to ΔT_m, ***r***-values and the *bulk crust/magma ratio* (M_a/M_{om}) may be predicted in small increments from Eq. (1) using appropriate thermodynamic constants of basalt and metapelite (C_m and C_{cr} are assumed to be identical and constant over the relevant temperature interval at 1500 J/kg per K; L_c and L_{cr} are 40000 and 35000 J/kg respectively; Spera, 2000) and the initial and final temperatures.

Fig. 2c and d illustrate ***r***-values and the *bulk crust/magma ratio* for energy-balanced AFC for the limiting case where all of the available heat is consumed by assimilation (EB100%) and when 75% (EB75%) and 50% (EB50%) is consumed by assimilation in a typical mid-crustal magma chamber that crystallizes over the temperature interval (1180–1025 °C) and assimilates metasedimentary country rock with an initial temperature of 450 °C. The model assumes that both restite material and the partial melt are heated to the temperature of the magma, and hence ΔT_{cr} decreases from 730 °C (1180–450) to 575 °C (1025–450) over the crystallization interval. This assumption is appropriate if the assimilated material consists of numerous small country rock xenoliths included in the magma chamber but not when the assimilated material derives from the contact metamorphic envelope itself. In the latter instance it is more realistic that the temperature of the restite country rock remains between that of its solidus (750–1000 °C) and the magma temperature, and only the partial melt has to be heated to the magma temperature. This would shift the *bulk crust/magma ratio* curves in Fig. 2d slightly upwards, and flatten the ***r***-curves in Fig. 2c, but not by very much. If no energy is lost to the surrounding host rocks (E_L=0, termed EB100% in Fig. 2c and d) (i.e. an unrealistic assumption that all the heat available is consumed by assimilation), the *bulk crust/magma ratio* reaches a maximum of 0.38 when the mass crystallized/initial mass of magma (M_c/M_{om}) is 1. The ***r***-value, which is represented by the tangent to the assimilation curves in Fig. 2d, changes in this case from 0.31 at the onset of crystallization to 0.45 for M_c/M_{om} of 1. In a more reasonable scenario, namely when a significant proportion of the energy is lost to the country rocks, the rate and amount of assimilation is obviously lower. For example, if half of the heat is lost to the envelope (E_L=0.5, termed EB50%), the *bulk crust/magma ratio* and ***r***-values are halved, so that, for example, when M_c/M_{om} is 0.5, M_a/M_{om}, the *bulk crust/magma ratio*, is 0.09 and ***r*** is 0.19 (Fig. 2c and d).

In an upper-crustal magma chamber, the potential for assimilation is reduced because the country rocks are cooler. If the initial country rock temperature is 200 °C and no energy is lost to the surrounding host rocks (E_L=0), the *bulk crust/magma ratio* is 0.28 for M_c/M_{om} of 1, and ***r*** increases from 0.24 at the onset of crystallization to 0.32 for M_c/M_{om} of 1 (not shown in Fig. 2). The reduction in temperature of the initial country rock from 450 °C in the mid-crustal case to 200 °C in the upper crustal case hence results in a 25% decrease in the amount of assimilation that is possible.

3.3. Constraints from volcanic and intrusive rocks

Attempts to constrain ***r*** in natural rock systems are rare. This is due to the difficulties of constraining *F*, the proportion of magma remaining during AFC in natural volcanic systems, which is necessary to solve the AFC equation for ***r*** (DePaolo, 1981). To circumvent this problem, Grove et al. (1988) and Aitcheson and Forrest (1994) suggested graphical solutions in which an average value for ***r*** is deduced from the intersection of trends for two or more elemental abundances or isotopic ratios in *F* (or *bulk crust/magma ratio*) versus ***r*** space. For example, Aitcheson and Forrest (1994) used Sr and Nd isotope ratios and argued that ***r*** is 0.08 and the *bulk crust/magma ratio* is 0.06 in the Upper Zone of the Lille Kufjord Intrusion, a mid-crustal layered gabbro that is assumed to have crystallised during AFC (Robins et al., 1991). The drawback of this solution, however, is that the rate and amount of assimilation cannot be monitored as a function of *F*. Similarly, Grove et al.

(1988) found that several incompatible trace-element concentrations in the Burnt Lava flow (Medicine Lake, California) overlap for $\boldsymbol{r}=1.35$ and $F=0.68$. To explain such a high $\boldsymbol{r}$ value, Grove et al. (1988) concluded that heat and mass transfer were separated in time and space, and that the Burnt Lava formed by mixing of a partial melt of granitic crust and a basaltic magma.

More recently, Tegner et al. (1999) adopted an alternative approach to constrain AFC processes in magma chambers using data from layered intrusions. In the mid-crustal Hasvik Layered Intrusion, Northern Norway, a 1200-m-thick sequence of cumulates crystallised by AFC processes without magma recharge. F was constrained from phase and cryptic layering, and $\boldsymbol{r}$ was then determined from the best fit of the model AFC curve to the Sr and Nd isotopic data. In this way, it was shown that the apparent $\boldsymbol{r}$-value was constant at 0.27 during almost 80% crystallization of a mantle-derived basaltic magma. In the following sections we apply this technique to two additional Norwegian layered intrusions, the Fongen–Hyllingen and Bjerkreim–Sokndal intrusions.

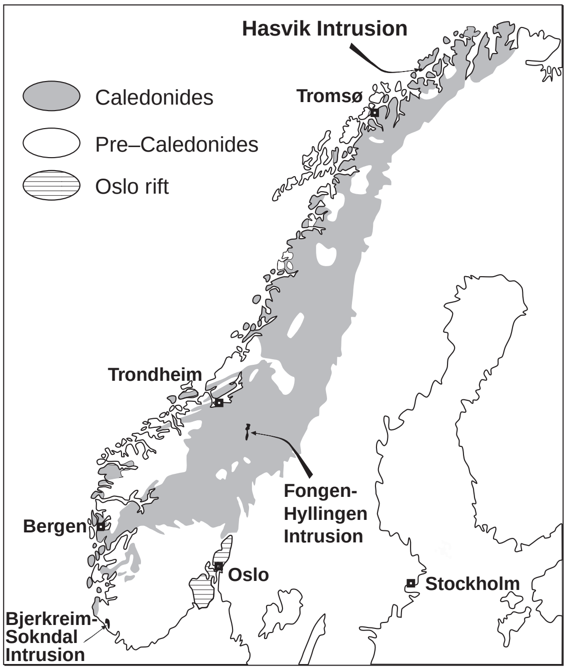

Fig. 3. Simplified geological map of Scandinavia showing the location of the Bjerkeim–Sokndal, Fongen–Hyllingen and Hasvik layered intrusions.

4. Geological background and Sr–Nd isotope data

4.1. The Fongen–Hyllingen layered intrusion

The 160 km^2 synorogenic Fongen–Hyllingen Intrusion is 426 ± 8 Ma old, was emplaced into folded metasediments and metabasalts at 3.5 ± 0.5 kbar, and is now located in the upper allochthon of the Caledonides, 60 km southeast of Trondheim, Norway (Fig. 3) (Wilson and Sørensen, 1996). The parental magma was basaltic-andesite with a moderate H_2O content, resulting in cumulus plagioclase (An_{57}), augite, and olivine (Fo_{73}) in the most primitive rocks followed by the appearance of low-Ca pyroxene and the disappearance of olivine, the appearance of Fe–Ti oxides, the re-appearance of olivine, and shortly thereafter the successive appearance of cumulus amphibole, apatite, biotite, zircon, quartz, alkali feldspar and allanite. The plagioclase reaches An_2 in the most evolved cumulates of quartz-bearing syenitic composition at the stratigraphic top of the intrusion. The cumulate stratigraphy can be correlated along strike for over 40 km, exceeds 4 km in thickness and displays systematic up-section changes in plagioclase An% and whole rock Sr_0 and εNd_0 (Fig. 4) (Sørensen and Wilson, 1995). On the basis of the cryptic layering and assuming that the magma was compositionally stratified with respect to both isotopes and elemental concentrations, Sørensen and Wilson (1995) divided the layered series into four stages representing from base to top: a basal reversal that developed during expansion of the chamber (I); concurrent magma recharge and fractional crystallization (IIA); fractional crystallization without concurrent recharge and assimilation (IIB); prolonged influx of primitive magma, magma mixing, and fractional crystallization (III); uninterrupted, closed-system fractional crystallization coupled with assimilation of country rocks (IVA); and finally fractional crystallization of evolved, contaminated magma without further assimilation (IVB). This paper focus on stage IVA, composed at the base of mafic cumulates containing relatively primitive plagioclases (An_{53}), together with the lowest Sr_0 (0.7035) and highest εNd_0 (+5.3) in the intrusion. The upper portion of the ~900 m thick stage IVA consists of

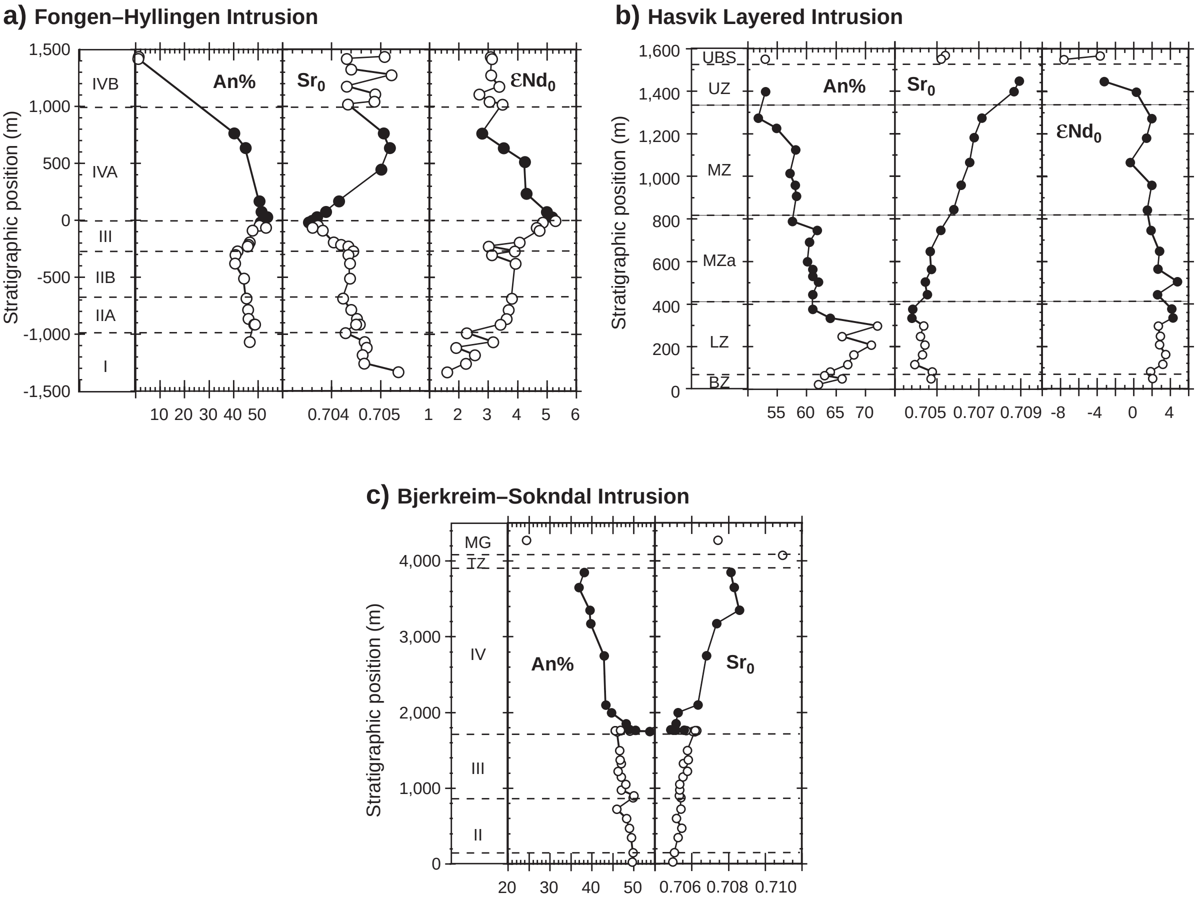

Fig. 4. Sr_0, εNd_0 and plagioclase An% in compiled stratigraphic sections of Fongen–Hyllingen (H2 section across the Hyllingen Series), Hasvik and Bjerkreim–Sokndal (Nonsknuten–Storeknuten section) layered mafic intrusions based on Sørensen and Wilson (1995), Tegner et al. (1999), and Nielsen et al. (1996), respectively. The filled symbols show the samples formed by concurrent assimilation and fractional crystallization that are modelled in this study.

evolved oxide-amphibole gabbros with An_{40}, with the highest whole rock Sr_0 (0.7052) and lowest εNd_0 (+2.8) of the intrusion (apart from somewhat lower εNd_0 and higher Sr_0 values developed in the basal reversal of stage I, as documented by Sørensen and Wilson (1995)). AFC modelling by Wilson et al. (1987) and Sørensen and Wilson (1995) showed that the assimilated material was a partial melt of local metapelitic country rocks. Sørensen and Wilson (1995) proposed that assimilation took place predominantly in the roof zone between stratified basic magma and an overlying buoyant layer of magma produced by partial melting of metapelitic country rocks. They inferred that downward transportation of roof melt to the crystallization front at the floor of the chamber took place by diffusion across double-diffusive interfaces, and as a result of periodic mixing of adjacent magma layers.

4.2. The Hasvik layered intrusion

The exposed part of the 700 Ma Hasvik layered intrusion occupies only 12 km^2 and is located at the southwestern tip of the island of Sørøy, northern Norway (Fig. 3) (Robins and Gardner, 1974; Tegner et al., 1999). A pronounced aeromagnetic anomaly suggests, however, that the intrusion is much larger and extends below the sea to the south. The intrusion is part of the Seiland Igneous Province, preserved within one of the nappes constituting the Middle

Allochton of the North Norwegian Caledonides. The Hasvik intrusion was emplaced into mid-crustal metasedimentary country rocks at 5–7 kbar. The parental magma was a tholeiitic basalt with 7.63 wt.% MgO and crystallized cumulus plagioclase, augite, and olivine. The 1600 m thick stratigraphic section is composed of a ~1500 m thick Layered Series overlying a thin Basal Zone and underlying an Upper Border Series (Fig. 4). The most primitive cumulates contain Fo_{78}, augite and An_{72} and are found at a stratigraphic height of 335 m within the Lower Zone. Below this level An% and εNd_0 increases and Sr_0 decreases upward reflecting magma recharge and mixing. Sr_0 of 0.7038 and εNd_0 of +4.3 in the most primitive cumulates at 335 m indicate that the parental magma was little contaminated. Low-Ca pyroxene appears and olivine disappears at the base of Middle Zone a, and Fe–Ti oxides and apatite appear respectively at the bases of Middle Zone b and the Upper Zone. In the interval between 335 and 1520 m, the stratigraphic changes in plagioclase An% (An_{72}–An_{52}), whole rock Sr_0 (0.7038–0.7089) and εNd_0 (+4.3 to −3.2) suggest concurrent assimilation and fractional crystallization uninterrupted by magma recharge (Fig. 4). Modelling carried out by Tegner et al. (1999) suggests that assimilation of the metasedimentary country rocks and fractional crystallization took place at a constant ratio ($\boldsymbol{r}$) of 0.27. The Hasvik Intrusion is thus one of the most contaminated layered intrusions known, and Robins and Gardner (1974) and Tegner et al. (1999) argued that the incorporation of innumerable metasedimentary slabs and flakes into the magma chamber, preserved as restite xenoliths in the cumulates, promoted contamination.

4.3. The Bjerkreim–Sokndal Layered Intrusion

The 230 km^2 Bjerkreim–Sokndal Layered Intrusion, 60 km southeast of Stavanger, Norway (Fig. 3), is 930–920 Ma old and was emplaced at depths corresponding to ~5 kbar into massif-type anorthosite plutons (~930 Ma) of the Rogaland Province as well as quartzo-feldspathic gneisses previously deformed and metamorphosed during the Sveconorwegian orogeny (Wilson et al., 1996). The gneisses were preheated to temperatures of 640–880 °C by the anorthosite plutons prior to the emplacement of the Bjerkreim–Sokndal Intrusion (Westphal et al., 2003). The intrusion is composed of an up to 7000 m thick Layered Series consisting of anorthosite, leuconorite, troctolite, norite, gabbronorite, jotunite, mangerite, quartz mangerite, and charnockite. In the Nonsknuten–Storeknuten area, the Layered Series, is ~4000 m thick and has been divided into 3 Macrocyclic Units each containing cumulates formed during a major recharge and mixing event followed by concurrent fractional crystallization and assimilation (Fig. 4). The parental magma was jotunitic (monzonoritic), an unusual magma-type rich in Ti, Fe and P, and low in calcium relative to basalt. Its crystallization sequence was also distinctive in that plagioclase is the first liquidus phase, ilmenite crystallized early and Ca-rich pyroxene only appeared as a cumulus mineral in evolved cumulates after magnetite and at about the same time as apatite. This crystallization sequence is consistent with an origin by partial melting of lower crustal rocks (Duchesne et al., 1999; Longhi et al., 1999), as supported by isotopic studies (Schiellerup et al., 2000). The highest-temperature cumulates are ilmenite troctolites with An_{53} and Fo_{77}, and the most evolved gabbronorites contain cumulus plagioclase (An_{37}), low- and high-Ca pyroxene, Fe-rich olivine (Fo_{46}), ilmenite, magnetite, and apatite. Nielsen et al. (1996) presented the Sr_0 and An% data shown in Fig. 4. Here we focus on a sampled stratigraphic profile, the Nonsknuten–Storeknuten section, through the 2200-m-thick Macrocyclic Unit IV (Fig. 4) that is the thickest and most completely developed unit located in the western flank of the intrusion. In this section, the most calcic plagioclases (An_{50}) and the lowest Sr_0 (0.7048) in the whole intrusion occur a few metres above the base of Macrocyclic Unit IV. In the overlying cumulates, plagioclase gradually changes to An_{37} and Sr_0 increases to 0.7086. As suggested for the Fongen–Hyllingen intrusion, Nielsen et al. (1996) concluded that crystallization in the Bjerkreim–Sokndal magma chamber took place at the bottom of a compositionally stratified magma overlain by a buoyant partial melt of country-rock gneisses from which material was transported downwards into the main magma body. In addition, Nielsen et al. (1996) pointed also to the importance of gneissic xenoliths sinking through the magma chamber as a means of transmitting assimilated material to crystallization front.

5. AFC modelling

5.1. Background and formalism

Bowen (1928), Wilcox (1954) and others have shown that assimilation in basaltic magma chambers is driven by the heat contained within the magma and cumulates, and the latent heat of crystallization as is expressed in the left-hand side of Eq. (1). In the energy-constrained examples of AFC discussed above (Fig. 2), crystallization provides approximately two-thirds of the heat released, while one-third originates from the magma. Later, DePaolo (1981) and Stewart and DePaolo (1990) described the changes in isotopic and elemental composition of magma during AFC processes. They showed that the change in isotopic ratio with mass crystallized is:

$$\mathrm{d}e_\mathrm{m}/\mathrm{d}M_\mathrm{c} = 1/M_\mathrm{m}[\boldsymbol{r}c_\mathrm{a}/c_\mathrm{m}(e_\mathrm{a} - e_\mathrm{m})] \tag{2}$$

and c_m changes with $\boldsymbol{r}$ and D_e according to:

$$\mathrm{d}c_\mathrm{m}/\mathrm{d}M_\mathrm{c} = 1/M_\mathrm{m}[\boldsymbol{r}(c_\mathrm{a}/c_\mathrm{m}) - c_\mathrm{m}(D_\mathrm{e} - 1)] \tag{3}$$

The symbols are defined in Table 1.

5.2. Application to layered intrusions

In well-exposed layered intrusions it is possible to constrain the mass proportions of cumulates and hence estimate the proportion of magma remaining (F) for samples collected systematically in stratigraphic sections, as has been done, for example, in the Kiglapait (Morse, 1979) and Skaergaard intrusions (Nielsen, 2004). Such constraints are the key to the modelling of crystallization and AFC processes because they allow direct comparison of theoretical models and data from natural rocks. For the Hasvik Layered Intrusion, Tegner et al. (1999) adopted this approach to constrain $\boldsymbol{r}$. First the location of individual samples was converted to F by assuming a linear relation with stratigraphic thickness and assuming that approximately 75% of the magma had crystallized when apatite appeared as a cumulus phase. The $\boldsymbol{r}$-value was then estimated by fitting Eq. (2) to the data. Below we adopt a similar approach to estimate $\boldsymbol{r}$ for the Fongen–Hyllingen and Bjerkreim–Sokndal layered intrusions.

6. Results of AFC modelling

6.1. The Fongen–Hyllingen Intrusion

The input parameters listed in Table 2 are taken from Sørensen and Wilson (1995), except that we assume that the average assimilated material had 200 p.p.m. Sr and 30 p.p.m. Nd, concentrations between those of the bulk metapelite and partial melts thereof (Wilson et al., 1987). The rationale behind this assumption is that only the initial partial melt can be assumed to have had an extremely high Nd/Sr as suggested by Wilson et al. (1987), and that the dilution effect of further melting of metapelite will lower Nd/Sr to an intermediate value. Stage IV is 1450 m thick (Fig. 4) and if it is assumed that the stratigraphic position of samples relate linearly to the

Table 2
Input parameters for the AFC modelling

	Fongen–Hyllingen	Hasvik	Bjerkreim–Sokndal
Parental magma			
Sr_0	0.7036[a]	0.7038[b]	0.7050[c]
Sr (p.p.m.)	205[d]	448[e]	530[f]
De (Sr)	0.95	0.95[b]	1.08[g]
$\varepsilon\mathrm{Nd}_0$	+5.4[a]	+4.3[b]	
Nd (p.p.m.)	11[d]	10[e]	
D_e (Nd)	0.29	0.29[b]	
Assimilated material			
Sr_0	0.7195[h]	0.7182[i]	0.7196[j]
Sr (p.p.m.)	200[k]	323[i]	447[j]
$\varepsilon\mathrm{Nd}_0$	−8.7[h]	−5.9[i]	
Nd (p.p.m.)	30[k]	34[i]	

[a] Most primitive and least contaminated cumulate rock (Sørensen and Wilson, 1995).

[b] Most primitive and least contaminated cumulate rock (Tegner et al., 1999).

[c] Most primitive and least contaminated cumulate rock (Nielsen et al., 1996).

[d] Concentration in mineral divided by the partition coefficient (Sørensen and Wilson, 1995).

[e] Chilled margin (sample CT5 from Tegner et al., 1999).

[f] Average composition of associated jotunitic dykes (Robins et al., 1997).

[g] Duchesne (1978).

[h] Average metapelite country rock (Sørensen and Wilson, 1995).

[i] Average wall rock metasediments (Tegner et al., 1999).

[j] Average adjacent sveconorwegian gneisses (Nielsen et al., 1996; Barling et al., 2000).

[k] Hypothetical mix between concentration in metapelite country rock and partial melt thereof (Wilson et al., 1987).

mass crystallised, F ranges from 1 to 0.46 for the modelled samples. Fig. 5a demonstrates that a constant $\boldsymbol{r}$-value of 0.12 gives the best fit to the Sr_0 and εNd_0 data. At the top of stage IVA, that is after 54% crystallization, the *bulk crust/magma ratio* is 0.08 and *the instantaneous crust/magma ratio* of the magma is 0.14 (Fig. 6).

6.2. The Hasvik Layered Intrusion

Using the input parameters listed in Table 2, and assuming that F is 0.15 at the top of the Upper Zone and relates linearly to stratigraphic position (Tegner et al., 1999), the AFC model closely fits the Sr_0 data for a constant $\boldsymbol{r}$-value of 0.27 (Fig. 5). However, the εNd_0 data are more scattered and generally lie above the AFC model curve. Tegner et al. (1999) ascribed this discrepancy to a secular decrease in Nd concentration in the material assimilated due to the progressive loss of incompatible Nd during partial melting of the country rock xenoliths, and perhaps slower diffusion of Nd relative to Sr. At the level of the uppermost sample, formed after almost 80% crystallization, the *bulk crust/magma ratio* is 0.28 and the magma had an *instantaneous crust/magma ratio* of 0.70 (Fig. 6).

6.3. The Bjerkreim–Sokndal Layered Intrusion

The Sr-concentration of the parental magma (530 p.p.m.) is constrained from the average composition of chilled margins (Robins et al., 1997), whereas Sr_0 (0.7050) is assumed to be that of the most primitive and least contaminated cumulates of the intrusion (Nielsen et al., 1996). The intrusion was emplaced into both massif-type anorthosite and gneisses but Nielsen et al. (1996) argued that the anorthosite is so refractory that the Bjerkreim–Sokndal magma would not have been capable of assimilating it and concluded that the assimilated material was mainly the country rock gneisses. Average values of 0.7196 for Sr_0 (Nielsen et al., 1996) and 447 p.p.m. for Sr (Barling et al., 2000) are assumed for these gneisses (Table 2). In the AFC model we assume that stratigraphic position within the 2200 m thick Macrocyclic Unit IV (Fig. 4) relates linearly to F and that F is 0.2 at the top. The rationale behind this assumption is that in Macrocyclic Unit IV, apatite started crystallizing when 37% of the magma had crystallized if F relates linearly to the stratigraphic column (Wilson et al., 1996), which is generally consistent with the P_2O_5 content of the preferred parental magma (0.8 wt.% P_2O_5, Robins et al., 1997) and expected apatite

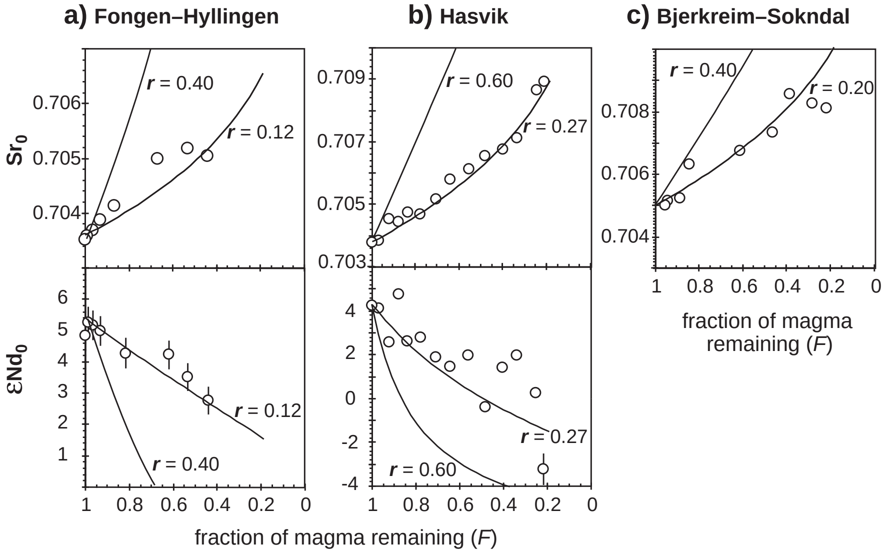

Fig. 5. AFC model curves compared to Sr_0 and eNd_0 data for the Fongen–Hyllingen, Hasvik, and Bjerkreim–Sokndal layered intrusions. Note that the abscissa value F, the fraction of magma remaining, differs from the abscissa in Fig. 2 (M_c/M_{om}) in that the mass of assimilated partial melt is taken into account in F.

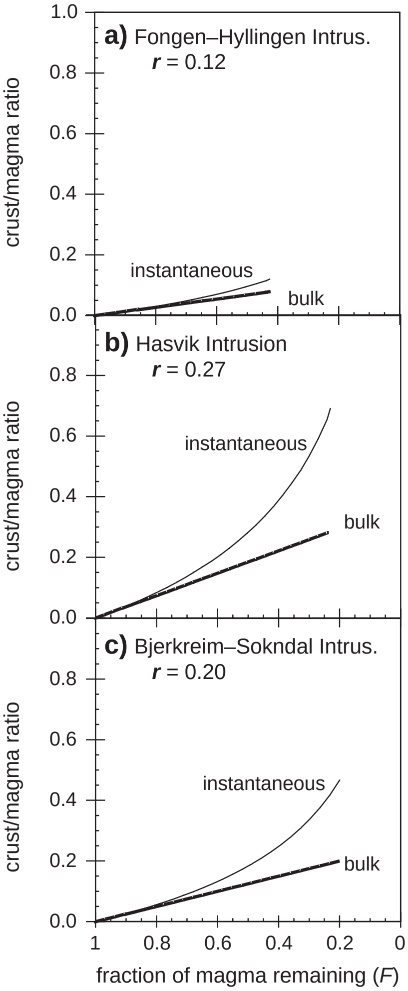

Fig. 6. Predicted *bulk* and *instantaneous crust*/*magma ratios* of the best-fit AFC models for the Fongen–Hyllingen, Hasvik, and Bjerkreim–Sokndal layered intrusions.

saturation at ~1.4 wt.% P_2O_5 (Cawthorn and Walsh, 1988), that is after 43% crystallization if P is perfectly incompatible. The assumption that F is 0.2 at the top of unit IV is based on the inference that the Transition Zone and mangerites represent the most evolved differentiation products (Fig. 4).

Fig. 5 illustrates that a constant $\boldsymbol{r}$ of 0.20 satisfies the Sr_0 data. A larger $\boldsymbol{r}$-value of, for example, 0.40, predicts a much steeper increase in Sr_0 than is apparent in the data. For an $\boldsymbol{r}$-value of 0.20, the level of the uppermost sample from Macrocyclic Unit IVA, where 80% of the unit had crystallized, corresponds to a *bulk crust*/*magma ratio* of 0.19 and an *instantaneous crust*/*magma ratio* of 0.46 (Fig. 6).

7. Discussion

7.1. Rate and amount of assimilation in layered intrusions

The models for concurrent assimilation and fractional crystallization presented for the Fongen–Hyllingen, Bjerkreim–Sokndal and Hasvik layered intrusions demonstrate that in large crustal magma chambers, the apparent relative rate of assimilation is to a first approximation constant in cumulate sequences up to 2 km thick and representing up to 80% crystallization. The $\boldsymbol{r}$-values of respectively 0.12, 0.20 and 0.27 estimated for the Fongen–Hyllingen, Bjerkreim–Sokndal and Hasvik intrusions (Fig. 5) are for basaltic–andesitic, jotunitic, and tholeiitic parental magmas. Compared to the $\boldsymbol{r}$-values and *bulk crust*/*magma ratios* derived from the energy balance, the Hasvik Intrusion falls close to the EB75% curve simulating a case where 75% of the heat available is consumed by the country rock involved in the AFC process (Fig. 2d). Clearly, a fraction of the heat available must inevitably be lost to the surrounding country rocks and refractory xenoliths (see below). We therefore argue that the Hasvik intrusion displays rates and amounts of assimilation that are close to the maximum possible in mid-crustal magma chambers.

7.2. Comparison with thermodynamic models

The observational evidence for constant $\boldsymbol{r}$ during AFC processes differs from the published thermodynamic simulations shown in Fig. 2. The $\boldsymbol{r}$-values initially above unity suggested from both MELTS (Reiners et al., 1995) and mineral dissolution models (Edwards and Russell, 1998) for primitive basaltic magma crystallizing only olivine cannot be compared directly to the $\boldsymbol{r}$-values of the magmas dealt with here as these were multisaturated. Reiners et al. (1995) and Edwards and Russell (1998) argue that the mass crystallized (per °C of cooling) is low for olivine alone (due to the steep liquidus surface) and results in $\boldsymbol{r}$-values above unity. Similarly, they argue that the sharp drop in $\boldsymbol{r}$ to 0.4–0.5 in the thermodynamic simulations (Fig. 2a) is due to a dramatic increase in mass crystallized when plagioclase and/or Ca-rich pyroxene joins olivine on the liquidus. Such discontinuities in the ***r***-value imply that the assimilation process is coupled to the topology of the relevant liquidus surfaces, but we find no evidence for this in the studied layered intrusions (Figs. 1 and 2). The ***r***-curves for multisaturated basalt in the MELTS and mineral dissolution models range between 0.4 and 0.5. That is 1.5 to 4 times higher than the ***r***-values obtained for the intrusions (Fig. 2) for similar initial conditions, that is magma at ~1200 °C and country rock initially at ~450 °C. It is also 25% or more higher than the maximum ***r***-value obtained from the energy-balanced calculation assuming that all the thermal energy released is consumed in the assimilation process (EB100% in Fig. 2). This discrepancy can be ascribed to the fraction of the crustal material, perhaps 0.35, that is assumed here to be heated and transformed into a refractory restite but not assimilated. Omitting this assumption in the energy-balanced calculation results in ***r***-values increasing from 0.44 to 0.48 with the ratio of mass crystallized to mass of original magma changing from 0 to 0.3 (not shown in Fig. 2c), which is similar to the ***r***-values of the MELTS and mineral dissolution models (Fig. 2a). As acknowledged by the authors, the thermodynamic simulations are end-member models (Reiners et al., 1995; Edwards and Russell, 1998; Spera and Bohrson, 2001) that define the maximum rate and amount of crustal assimilation possible in magma chambers under particular circumstances, whereas our intrusion data and models record AFC processes as they actually occurred in nature.

The ***r***-values and *bulk crust*/*magma ratio* predicted by the EC-AFC model (Spera and Bohrson, 2001) are very different to those inferred from the layered intrusions, our energy-balanced calculations, MELTS and the mineral dissolution model (Fig. 2). The reason for this is that the EC-AFC model assumes that the assimilant is derived exclusively from the thermal aureole and that all the crustal material is heated *before* assimilation begins. The data from the intrusions presented here demonstrates that this assumption is not valid in real magma chambers.

One feature that emerges from the comparison in Fig. 2 is that whereas the MELTS and mineral dissolution simulations and the energy-balanced calculation indicate that ***r*** gradually increases with crystallization, the intrusion models suggest that ***r*** is near-constant over large crystallization intervals (Fig. 5). The reason why ***r*** increases with crystallization in our energy-balanced calculation is that, with falling magma temperature, less energy is required to heat the crustal material to the temperature of the magma (see Section 3.2). The partial melt assimilated must be heated to the temperature of the magma in order to equilibrate and mix with it, but it is plausible that the restite country rock involved in the AFC process is heated to a somewhat lower temperature. It is therefore possible that the rate by which ***r*** increases with crystallization is less than shown by the EB curves in Fig. 2c, but the energy-balance predicts that ***r*** ought to increase slightly with falling temperature. The intrusion data would allow for slight increases in ***r*** with prolonged crystallization, for example, in the Sr_0 data for the Hasvik intrusion (Fig. 5). However, as a first approximation, the intrusion data shows that ***r*** was constant.

7.3. *The significance of country-rock xenoliths*

Innumerable xenoliths of the local country rocks are enclosed in the three studied intrusions. Some examples are shown in Fig. 7. In the Fongen–Hyllingen intrusion, large raft-like metabasaltic inclusions dominate but there are also numerous metapelitic inclusions, consistent with the proportion of these rock types in the adjacent host rocks (Habekost and Wilson, 1989). Some of the metabasaltic inclusions are large slabs (up to 1500 × 100 m) concordant with modal layering; they comprise up to 22% of the Layered Series. Habekost and Wilson (1989) observed that the rafts are connected in a three-dimensional framework and concluded they are essentially in situ inclusions enveloped by the cumulates. The metabasaltic inclusions are metamorphosed to equigranular pyroxene and/or olivine granofels, and locally contain a small proportion of leucosomes representing partial melts (Habekost and Wilson, 1989). The Sr-isotopic composition of the metabasaltic country rocks is similar to the parental magma of the intrusion (Wilson et al., 1987; Sørensen and Wilson, 1995). Hence, minor contamination by assimilation of partial melts from metabasalt rafts would not be readily detected in Sr (and Nd) isotopic ratios. The metapelitic xenoliths

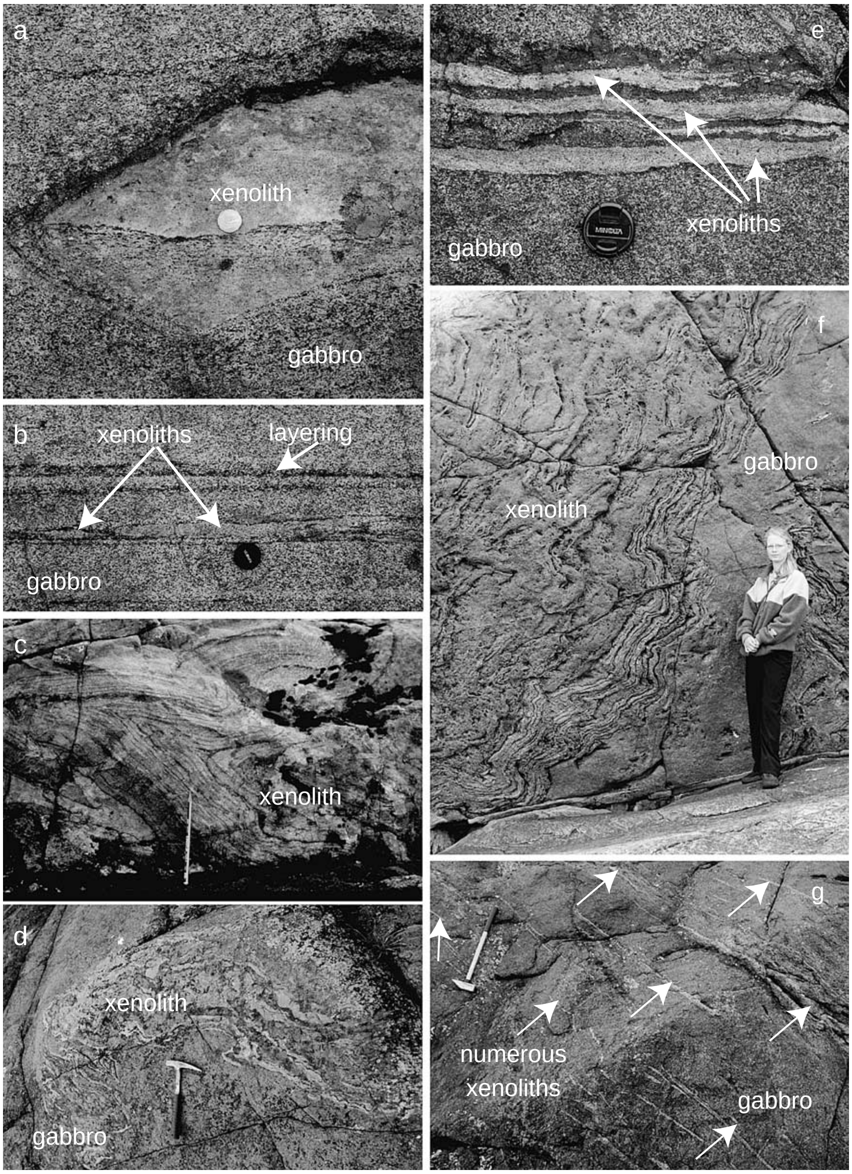

Fig. 7. Examples of country rock xenoliths included in the studied layered cumulates: (a) Angular gneiss block with relict banding enclosed in ilmenite–norite, megacyclic unit II, Teksetjørni, Bjerkreim–Sokndal layered intrusion (coin for scale); (b) Thin flakes of gneissic material recrystallized to pyroxene hornfels mineralogy enclosed in layered ilmenite–norite, megacyclic unit II, Teksetjørni, Bjerkreim–Sokndal layered intrusion (lens cap for scale); (c) Metre-sized metapelite inclusion showing relict regional isoclinal folding enclosed in layered cumulates (not shown) of the Fongen mountain, Fongen–Hyllingen layered intrusion (hammer shaft for scale). The block displays pyroxene hornfels facies mineralogy with Ca-poor pyroxene-rich dark bands; (d and f) Large metasedimentary xenoliths showing relict regional folding enclosed in apatite–oxide–norite of the Upper Zone of the Hasvik layered intusion; (e and g) Numerous thin flakes of metasedimentary country rocks, now pyroxene hornfels, enclosed in apatite–oxide–norite of the Upper Zone of the Hasvik layered intusion. The dark layers in (e) are rich in Ca-poor pyroxene.

in Fongen–Hyllingen range from very small flakes to slabs several hundreds of metres in length and some exhibit relict regional folds (Fig. 7c). They contain pyroxene hornfels facies mineral assemblages dominated by plagioclase, quartz, and Ca-poor pyroxene.

In the Bjerkreim–Sokndal intrusion there are numerous xenoliths within the Layered Series. Their compositions reflect the lithology of the adjacent country rocks and comprise anorthosite, leuconorite, mafic granulite, amphibolite, leucogranite, coarse-grained quartzite and quartzo-feldspathic gneisses. Xenoliths of anorthosite and leuconorite are extremely abundant and vary widely in size from fragments a few cm in diameter to blocks up to 600 m long and 350 m broad. Locally there are large elongated enclaves of anorthosite, some more than 1.5 km long. Xenoliths of anorthosite and leuconorite are medium to very coarse-grained slabs or blocks that vary from angular to rounded. The margins of xenoliths are sharp and commonly exhibit narrow mafic rinds consisting of coarse-grained orthopyroxene and ilmenite. Rarely, small xenoliths have embayed margins that suggest advanced magmatic corrosion. Internally, the anorthosites and leuconorite xenoliths are either massive, foliated or banded due to variations in modal composition or grain size. The foliations in adjacent xenoliths generally have different orientations, showing that deformation took place before incorporation into the magma chamber. In larger xenoliths fresh plagioclase feldspar is commonly pink or violet in colour. Leuconorites generally exhibit subophitic textures, with tabular feldspar up to 10 cm long and interstitial orthopyroxene and ilmenite. Some xenoliths contain plagioclase and/or orthopyroxene megacrysts. The gneiss xenoliths range from flakes that are up to a few centimetres thick and up to 0.5 m long (Fig. 7b) to metre- to tens of metre-sized angular blocks or slabs with alternating bands of charnockitic composition, mafic granulite and coarse-grained blue quartz (Fig. 7a). The thin flakes are generally granofels composed mainly of plagioclase, Ca-poor pyroxene and quartz, and may be difficult to distinguish from the noritic host cumulates in other than superb exposures. They are ubiquitous in the Layered Series.

The Hasvik intrusion was emplaced into migmatitic, banded metasediments that had been metamorphosed and folded prior to magma emplacement (Roberts, 1974; Robins and Gardner, 1974). Their typical mineral assemblage is quartz, K-feldspar, plagioclase, garnet, biotite and sillimanite. Centimetre- to metre-thick bands represent arkosic sandstone, pelite, quartzite, and calc-silicate protoliths. In the up to 500 m wide thermal aureole, geothermobarometry and leucosomes representing partial melts indicate peak metamorphic temperatures of least 875 °C at pressures of 6–7.5 kbar (Tegner et al., 1999). Innumerable metasedimentary xenoliths occur within the Layered Series (Robins and Gardner, 1974; Tegner et al., 1999) and are particularly abundant in the Upper Zone where they locally make up 40% by volume. In the Middle Zone they comprise less than 5% and they are rare in the Lower Zone. The shapes and sizes of xenoliths vary widely (Fig. 7d–g). The most common types are 10–100 cm long and 1–5 cm thick rafts that are paler coloured than the host gabbro (Fig. 7e and g). These xenoliths are thoroughly transformed into pyroxene hornfels facies dominated by plagioclase, Ca-poor pyroxene (generally inverted pigeonite), and quartz (Robins and Gardner, 1974; Tegner et al., 1999). In the Upper Zone, there are abundant larger rafts and angular blocks up to tens of metres across that preserve regional folds (Fig. 7d and f).

The abundance of inclusions in the three studied layered intrusions suggests that interaction between xenoliths and magma is the key to AFC processes. Pivotal are the initial temperature, composition, size, and abundance of xenoliths. In Section 3.2 we showed that lowering the initial temperature of the country rocks, for example from 450 °C in the mid-crust to 200 °C in the upper crust, results in a reduction of 25% in the possible rate and amount of assimilation. The effect of abundant small xenoliths is obvious in greatly increasing the surface to volume ratio and hence promoting contamination. The important role played by the composition of the country xenoliths is clearly demonstrated in the studied intrusions. In the Hasvik intrusion, the xenoliths are composed almost exclusively of metasedimentary rocks that, apart from the quartzites, would yield a large fraction of partial melt when heated to magmatic temperatures (possibly 65% as discussed above) and very extensive contamination. In the Bjerkreim–Sokndal and Fongen–Hyllingen intrusions, on the other hand, a large proportion of the xenoliths are anorthositic or metabasalt that acted merely as heat sinks and produced little or no partial melt. Assimilation of metasediments and gneiss in these two cases is therefore expected to have been less effective. Further, the preheating of the gneiss host rocks to the Bjerkreim–Sokndal intrusion to 640–880 °C (Westphal et al., 2003) would have resulted in dehydration reactions and assimilation therefore would have required higher temperatures than for assimilating hydrous gneiss xenoliths. We conclude that the composition of xenoliths is the main reason for the different rates and amounts of assimilation in the Fongen–Hyllingen ($\boldsymbol{r}=0.12$), Bjerkreim–Sokndal ($\boldsymbol{r}=0.20$), and Hasvik ($\boldsymbol{r}=0.27$) magma chambers.

7.4. Implications for the thermal evolution of magma chambers

A startling implication of the results from this study is that up to 75% of the heat available during crystallization is absorbed by the heating and melting of xenoliths within the magma chambers themselves. After crystallization was completed heat from the intrusions dissipated into the adjacent country rocks. During crystallization in the chambers, the heat capacity of the magma over the crystallisation interval and the latent heat of crystallization make up, respectively, one-third and two-thirds of the heat available. It therefore appears that in the Hasvik magma chamber, the heat absorbed by xenoliths roughly equals the latent heat of crystallization plus a little of the heat contained in the magma. This implies that the heat lost to the surrounding country rocks, measured in J/°C of cooling, was more or less constant from magma emplacement to the cooling to the ambient temperature of the country rocks.

Abundant xenoliths with a high surface area in a magma chamber imply an increased cooling rate, especially if the xenoliths melt. This, in turn, causes higher rates of crystallisation than would have resulted from heat-loss through the country rocks alone.

7.5. Assimilation processes in magma chambers: role of xenoliths and compositionally zoned magma

The inference that $\boldsymbol{r}$ is apparently constant through thick layered sequences formed in chambers without magma recharge must indicate that AFC is a steady-state process that is most likely governed by the thermal balance and kinetics. In this section we discuss how this bears on physical processes in magma chambers, in particular where assimilation takes place and how the contaminant is transmitted to the magma and the cumulates.

There are several ways in which the isotopic signature of the country rocks may be transmitted to the magma: (i) bulk digestion; (ii) mixing with partial melts; (iii) chemical diffusion; (iv) isotopic self-diffusion. Given that large layered intrusions, such as the ultramafic and mafic portions of the Bushveld Complex, crystallized within less than 200000 years (Cawthorn and Walraven, 1998), chemical diffusion can be ruled out as being an important mechanism. However, Stewart and DePaolo (1992) found that more rapid isotopic self-diffusion of Sr than Nd could explain the decoupling of Sr and Nd isotopic ratios in the uppermost cyclic unit of the Muskox Complex. For the Fongen–Hyllingen and Hasvik intrusions, both Sr and Nd isotopes give similar $\boldsymbol{r}$-values in AFC models and are not consistent with isotopic self-diffusion being the governing process. However, the dispersion of data around the modelled AFC curves (Fig. 5) may reflect the minor effect of isotopic self-diffusion. The presence of abundant country-rock xenoliths in the studied layered intrusions (Fig. 7) argues against bulk digestion, unless an even larger number of xenoliths were completely dissolved. We therefore conclude that contamination by partial melts derived from the country rocks is the most plausible means of assimilation in basaltic magma chambers.

A commonly held belief is that a mixture of partial melt derived from the country rock and evolved resident magma forms a buoyant layer of melt at the roofs of magma chambers (Campbell and Turner, 1987; Stewart and DePaolo, 1990, 1992; Sørensen and Wilson, 1995; Nielsen et al., 1996). In this model, the transport of roof melt, or its isotopic signature, to the crystallization front at the floor of the chamber could take place by diffusion across double diffusive interfaces and by mixing caused by density equalisation of adjacent magma layers.

Studies of the Vandfaldsdalen macro-dyke, East Greenland, have, however, shown that exchange between granophyric roof melt and underlying basalt was minimal (Geist and White, 1994). Likewise, Tegner et al. (1999) concluded that the distinct isotopic composition of the Upper Border Series (Fig. 4) ruled out contamination from a roof melt in the Hasvik magma chamber. Instead, Tegner et al. (1999) proposed that neutrally buoyant country rock xenoliths were spalled off the roof of the chamber during magma emplacement and therefore concentrated in the upper part of the chamber. Only after extraction of partial melts and recrystallization would the density of the country rock xenoliths increase sufficiently to allow them to sink to the floor of the chamber.

There is good evidence in both the Bjerkreim–Sokndal and Fongen–Hyllingen intrusions (and other layered intrusions and volcanic successions) for compositionally stratified magma chambers (Wilson and Sørensen, 1996; Wilson et al., 1996). In such chambers, the density of the magma increases downward. We therefore envisage that xenoliths may sink slowly, and perhaps in steps, due to a delicate interplay between the densities of the xenoliths, that secularly increase due to partial melting and recrystallization, and the density gradient of the magma. This would allow adequate time for the xenoliths to react with magma simultaneously across the entire chamber, as is indicated by the recrystallized xenoliths in the studied layered intrusion (Fig. 7). In the Fongen–Hyllingen intrusion, Wilson et al. (1987) showed that Sr_0 increases laterally towards a metapelitic country rock xenolith and concluded that xenoliths resulted in local contamination of the cumulates.

We surmise that assimilation of partial melts derived from country rock xenoliths was the dominant process in the studied intrusions. The slow sinking of near-neutrally buoyant xenoliths is an effective means of transmitting country rock material from the roof to the crystallization front at the floor of the chamber. Due to the near-neutral buoyancy of the xenoliths and their likely origin in the roof, xenoliths are commonly most abundant in the upper portion of a magma chamber, which is also the most contaminated part of the intrusions.

8. Summary and conclusions

Layered mafic intrusions provide useful constraints on the rates and amounts of assimilation that have taken place in magma chambers and insights into the physical means by which it took place. In our view, inferences from layered intrusions are superior to those derived from thermodynamic models and volcanic successions because thick layered cumulate sequences provide a direct and continuous record of prolonged assimilation and fractional crystallization. From our studies of the Fongen–Hyllingen, Hasvik, and Bjerkreim–Sokndal intrusions it is concluded that:

(1) The ratio of the rate of mass assimilated to mass crystallized, ***r*** in the AFC formulation (DePaolo, 1981), ranges from ~0.1 to ~0.3 in basaltic and jotunitic magma chambers crystallizing gabbroic or noritic cumulates in the middle crust. These values are supported by calculations of the heat released in crystallization and cooling of basalt, and the energy consumed in heating and melting country rocks. The maximum limit for ***r***, that is when all the available heat is consumed by assimilation, range from 0.31 at the onset of crystallization to 0.37 after 50% crystallization. Obviously, some fraction of the energy released must be lost to the surrounding country rocks. Hence, ***r***-values in excess of 0.3 are unrealistic in magma chambers crystallizing gabbroic or noritic cumulates.

(2) The ***r***-value is apparently constant in layered cumulate sequences up to 2 km thick and representing up to 80% crystallization. We estimate ***r***-values of 0.12, 0.20, and 0.27 for respectively the Fongen–Hyllingen, Bjerkreim–Sokndal, and Hasvik intrusions. Such constant rates for assimilation demonstrate that AFC was a steady-state process. This was a consequence of the ready availability of fusible country-rock xenoliths, providing an internal heat sink that played a major role in regulating the rate of crystallisation. The extreme ***r***-value inferred for the Hasvik magma chamber suggests that heating and melting of fusible xenoliths absorbed 75% of the heat released from the magma.

(3) The total amount of assimilation, the *bulk crust/magma ratio*, reaches values of 0.08, 0.19 and 0.28 in the most contaminated samples of the Fongen–Hyllingen, Bjerkreim–Sokndal and Hasvik intrusions, respectively. The *instantaneous crust/magma ratio* in the magmas from which the most contaminated samples of the

three intrusions crystallized are 0.14, 0.46, and 0.70 respectively.

(4) The abundance of fusible country rock xenoliths in the three intrusions suggests that they played a major role in magma contamination in large magma chambers. Assimilation was promoted by the large surface areas of the xenoliths. The metasedimentary and gneissic xenoliths are generally thoroughly transformed into noritic compositions representing high-temperature restites remaining after the extraction of partial melts. In contrast to the contaminating effect of metasedimentary xenoliths, refractory country rock xenoliths such as metabasalt (present in abundance in the Fongen–Hyllingen Intrusion) and anorthosite/leuconorite (present in abundance in Bjerkreim–Sokndal Intrusion) acted only as heat sinks. They decreased the heat available for the assimilation of metasedimentary and gneissic country rocks and simultaneously increased the rate of crystallisation. This is suggested as the main reason for the lower rates and amounts of assimilation in the Fongen–Hyllingen and Bjerkreim–Sokndal magma chambers relative to Hasvik.

(5) Similar ***r***-values are obtained from modelling of both Sr and Nd isotopic ratios, indicating that assimilation is principally a result of digestion of large-fraction partial melts. Selective, diffusion-controlled assimilation is, if effective at all, a process of secondary importance.

(6) Suspension of neutrally buoyant xenoliths or slow sinking of xenoliths spalled off from the roof of a chamber through a density- and compositionally stratified magma are effective means of transmitting country rock material to the crystallization front at the chamber floor.

Acknowledgments

We are very grateful to Jean-Clair Duchesne for many years of fruitful cooperation and to Jacqueline Vander Auwera for arranging a symposium and for editing this volume. Thoughtful referee reports by H. Martin and E. Mathez helped to clarify the manuscript. This study is supported by the Danish Natural Science Research Council grants 21-01-0297 and 21-01-0495 to CT and JRW.

References

Aitcheson, S.J., Forrest, A.H., 1994. Quantification of crustal contamination in open magmatic systems. Journal of Petrology 35, 461–488.

Barling, J., Weis, D., Demaiffe, D., 2000. A Sr-, Nd- and Pb-isotopic investigation of the transition between two megacyclic units of the Bjerkreim–Sokndal layered intrusion, south Norway. Chemical Geology 165, 47–65.

Bowen, N.L., 1928. The Evolution of Igneous Rocks. Princeton University Press. 322 pp.

Campbell, I.H., Turner, J.S., 1987. A laboratory investigation of assimilation at the top of a basaltic magma chamber. Journal of Geology 95, 155–172.

Cawthorn, R.G., Walraven, F., 1998. Emplacement and crystallization time for the Bushveld Complex. Journal of Petrology 39, 1669–1687.

Cawthorn, R.G., Walsh, K.L., 1988. The use of phosphorous contents in yielding estimates of the proportion of trapped liquid in cumulates of the Upper Zone of the Bushveld Complex. Mineralogical Magazine 52, 81–89.

Coogan, L.A., Mitchell, N.C., O'Hara, M.J., 2003. Roof assimilation at fast spreading ridges: an investigation combining geophysical, geochemical, and field evidence. Journal of Geophysical Research 108.

DePaolo, D.J., 1981. Trace element and isotopic effects of combined wallrock assimilation and fractional crystallization. Earth and Planetary Science Letters 53, 189–202.

Duchesne, J.C., 1978. Quantitative modeling if Sr, Ca, Rb, and K in the Bjerkreim–Sokndal Layered Lopolith (S.W. Norway). Contributions to Mineralogy and Petrology 66, 175–184.

Duchesne, J.C., Liégeois, J.P., Vander Auwera, J., Longhi, J., 1999. The crustal tongue melting model and the origin of massive anorthosites. Terra Nova 11, 100–105.

Edwards, B.R., Russell, J.K., 1998. Time scales of magmatic processes: new insights from dynamic models for magmatic assimilation. Geology 26, 1103–1106.

Geist, D., White, C., 1994. Assimilation and fractionation in adjacent parts of the same magma chamber: Vandfaldsdalen macrodike, East Greenland. Contributions to Mineralogy and Petrology 116, 92–107.

Grove, T.L., Kinzler, R.J., Baker, M.B., Donelly-Nolan, J.M., Lesher, C.E., 1988. Assimilation of granite by basaltic magma at Burnt Lava flow, medicine Lake Volcano, northern California: decoupling of heat and mass transfer. Contributions to Mineralogy and Petrology 99, 320–343.

Habekost, E.M., Wilson, J.R., 1989. Raft-like metabasaltic inclusions in the Fongen–Hyllingen Layered Intrusive Complex, Norway, and their implications for magma chamber evolution. Journal of Petrology 30, 1415–1441.

Longhi, J., Vander Auwera, J., Fram, M.S., Ducehsne, J.C., 1999. Some phase equilibrium constraints on the origin of Proteorozoic (massif) anorthosites and related rocks. Journal of Petrology 40, 339–362.

Michael, P.J., Cornell, W.C., 1998. Influence of spreading rate and magma supply on crystallization and assimilation beneath mid-ocean ridges: evidence from chlorine and major element chemistry of mid-ocean ridge basalt. Journal of Geophysical Research 103, 18325–18356.

Morse, S.A., 1979. Kiglapait geochemistry: I: Systematics, sampling, and density. Journal of Petrology 20, 555–590.

Nielsen, T.F.D., 2004. The shape and volume of the Skaergaard intrusion, Greenland: implications for mass balances and bulk composition. Journal of Petrology 45, 507–530.

Nielsen, F.M., Campbell, I.R., McCulloch, M., Wilson, J.R., 1996. A strontium isotopic investigation of the Bjerkreim–Sokndal layered intrusion, Southwest Norway. Journal of Petrology 37, 171–193.

Reiners, P.W., Nelson, B.K., Ghiorso, M.S., 1995. Assimilation of felsic crust by basaltic magma: thermal limits and extents of crustal contamination of mantle-derived magmas. Geology 23, 563–566.

Roberts, D., 1974. Hammerfest. Beskrivelse til det 1:250.000 berggrundsgeologiske kart. Norges Geologisk Tidskrift 301, 1–66.

Robins, B., Gardner, P., 1974. Synorogenic layered basic intrusions in the Seiland petrographic province, Finnmark. Norges Geologiske Undersøkelse Bulletin 312, 91–130.

Robins, B., Gading, M., Yurdakul, M., Aitcheson, S.J., 1991. The origin of macrorhythmic units in the Lower Zone of the Lille Kufjord Intrusion, northern Norway. Norske Geologiske Undersøgelser Bulletin 420, 13–50.

Robins, B., Tumyr, O., Tysseland, M., Garmann, L.B., 1997. The Bjerkreim–Sokndal Layered Intrusion, Rogaland, SW Norway: evidence from marginal rocks for a jotunite parent magma. Lithos 39, 121–133.

Schiellerup, H., Lambert, D.D., Prestvik, T., Robins, B., McBride, J.S., Larsen, R.B., 2000. Re–Os isotopic evidence for a lower crustal origin of massif-type anorthosites. Nature 405, 781–784.

Sørensen, H.S., Wilson, J.R., 1995. A strontium and neodymium isotopic investigation of the Fongen–Hyllingen layered intrusion, Norway. Journal of Petrology 36, 161–187.

Spera, F.J., 2000. Physical properties of magma. In: Sigurdsson, H. (Ed.), Encyclopedia of Volcanoes. Academic Press, New York, pp. 171–190.

Spera, F.J., Bohrson, W.A., 2001. Energy-constrained open-system magmatic processes: I. General model and energy-constrained assimilation and fractional crystallization (EC-RAFC) formulation. Journal of Petrology 42, 999–1018.

Stewart, B.W., DePaolo, D.J., 1990. Isotopic studies of processes in mafic magma chambers: II. The Skaergaard Intrusion, East Greenland. Contributions to Mineralogy and Petrology 104, 125–141.

Stewart, B.W., DePaolo, D.J., 1992. Diffusive isotopic contamination of mafic magma chambers by coexisting silicic liquid in the Muskox Intrusion. Science 255, 708–711.

Taylor, H.P., Giannetti, B., Turi, B., 1979. Oxygen isotope geochemistry of the potassic igneous rocks from the Roccamonfina volcano, Roman comagmatic region, Italy. Earth and Planetary Science Letters 46, 81–106.

Tegner, C., Robins, B., Reginiussen, H., Grundvig, S., 1999. Assimilation of crustal xenoliths in a basaltic magma chamber: Sr and Nd isotopic constraints from the Hasvik layered intrusion, Norway. Journal of Petrology 40, 363–380.

Vielzeuf, D., Holloway, J.R., 1988. Experimental determination of the fluid-absent melting relations in the pelitic system. Contributions to Mineralogy and Petrology 98, 257–275.

Westphal, M., Schumacher, J.C., Boschert, S., 2003. Role of magmatic heat sources at the Rogaland Anorthosite Complex in southwestern Norway. Journal of Petrology 44, 1145–1162.

Wilcox, R.E., 1954. Petrology of Paricutin volcano, Mexico. Geological Survey Bulletin 965-C, 281–353.

Wilson, J.R., Sørensen, H.S., 1996. The Fongen–Hyllingen layered intrusive complex, Norway. In: Cawthorn, R.G. (Ed.), Layered Intrusions. Elsevier Science, pp. 303–330.

Wilson, J.R., Menuge, J.F., Pedersen, S., Engel-Sørensen, O., 1987. The southern part of the Fongen–Hyllingen layered mafic complex, Norway: emplacement and crystallization og compositionally stratified magma. In: Parsons, I. (Ed.), Origins of Igneous Layering. Reidel, Dordrecht, pp. 145–185.

Wilson, J.R., Robins, B., Duchesnes, J.C., Nielsen, F.M., 1996. The Bjerkreim–Sokndal layered intrusion, Southeast Norway. In: Cawthorn, R.G. (Ed.), Layered Intrusions. Elsevier Science, pp. 231–255.